ACS OMEGA

Open Access

This article is licensed under CC-BY-NC-ND 4.0

http://pubs.acs.org/journal/acsodf

Article

Ultrasound-Triggered Amoxicillin Release from Chitosan/Ethylene Glycol Diglycidyl Ether/Amoxicillin Hydrogels Having a Covalently Bonded Network

Tu Minh Tran Vo, Pranut Potiyaraj, Patricia del Val, and Takaomi Kobayashi*

Cite This: *ACS Omega* 2024, 9, 585−597

Read Online

ACCESS | Metrics & More | Article Recommendations

ABSTRACT: An antibiotic release system triggered by ultrasound (US) was investigated using chitosan (CS)/ethylene glycol diglycidyl ether (EGDE) hydrogel carriers with amoxicillin (Amox) drug. Different CS concentrations of 1.5, 2, 2.5, and 3 wt % were gelled with EGDE and Amox was entrapped in the hydrogel carrier; the accelerated release was observed as triggered by 43 kHz US exposure at different US output powers ranging from 0 to 35 W. Among these CS hydrogel systems, the degree of accelerated Amox release depended on the CS concentration for the hydrogelation and the matrix with 2 wt % CS exhibited efficient Amox release at 35 W US power with around 19 μg/mL. The drug released with time was fitted with Higuchi and Korsmeyer−Peppas models, and the enhancement was caused by US aiding drug diffusion within the hydrogel matrix by a non-Fickian diffusion mechanism. The US effect on the viscoelasticity of the hydrogel matrix indicated that the matrix became somewhat softened by the US exposure to the dense hydrogels for 2.5 and 3% CS/EGDE, while the degree of softening was slightly marked in the CS/EGDE hydrogels prepared with 1.5 and 2% CS concentration. Such US softening also aided drug diffusion within the hydrogel matrix, suggesting an enhanced Amox release.

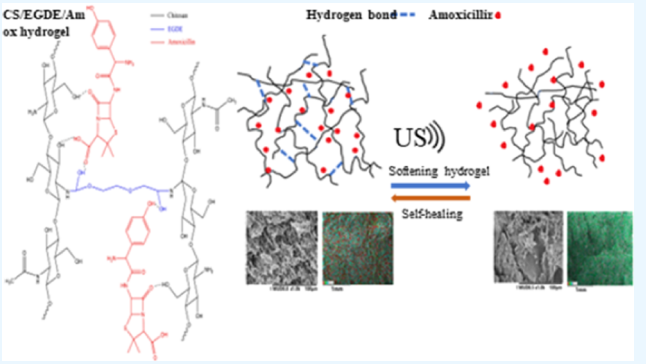

1. INTRODUCTION

Drug delivery systems (DDSs) have been developed to increase the effectiveness of drug delivery to the treatment site and to minimize drug toxicity due to drug overdose.[1] Drug side effects as a result of overdose can be optimally maintained while drug release is controlled to reduce fluctuations in its concentration. These characteristics made it possible to be targeted to specific tissues or cells, allowing for more effective treatment of specific conditions.[2] Over the past few years, numerous researchers have dedicated substantial effort to the comprehensive exploration of biomaterials designed for drug delivery. Their objective is to create and enhance polymeric substances that fulfill the specific requirements of biomedical applications. Polymer drugs, in which the matrix and drug are integrated, have often been used in the development of DDS systems by using a drug-loaded matrix like a hydrogel with high water retention in such hydrogel matrices, which consists of a three-dimensional network of hydrophilic polymers. Particularly, the large amounts of water in the matrix[3] endow it with a remarkable affinity, and the advantage of the swelling matrix is its body friendliness. Also, biomass polymer hydrogels have recently been the focus of attention in the selection of materials, especially in terms of biocompatibility.[4] Because of their high biocompatibility,[5] hydrophilic biomass polymers have received much attention and use.[6,7] Among them, chitosan (CS) is a water-soluble biomass polymer consisting of β-(1−4)-2 acetamido-D-glucose and β-(1−4)-2-amino-D-glucose units sourced from crustacean crabs[8] that has demonstrated tremendous potential because of its wound care property and the features of nontoxicity and antimicrobial activity. But, because of the water-soluble properties, hydrogelation is accompanied by a reaction with cross-linking agents. There have been several studies on the DDS matrix as described below. Generally, the important pathway of the cross-linking could enhance the chemical stability of hydrogel matrices formed with CS aqueous solution and glutaraldehyde[9] or epichlorohydrin,[10] becoming a crucial factor. In such cases, it is essential to select a water-soluble material with functional groups that are biocompatible for the cross-linked part as well as chitosan. Ethylene glycol diglycidyl ether (EGDE) has recently attracted a lot of attention as an effective option to CS

Received: August 21, 2023
Revised: November 17, 2023
Accepted: November 24, 2023
Published: December 19, 2023

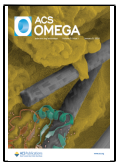

© 2023 The Authors. Published by American Chemical Society

hydrogelation due to its nontoxicity compared to glutaraldehyde, water solubility, and bifunctional diepoxy groups[11] having the ability of cross-linking with the amino groups ($-NH_2$) of the D-glucosamine units of the CS biopolymer,[12] improving its mechanical and elastic properties due to the covalent bonding of EGDE with CS. Recently, to increase the efficiency of sustained drug release, smart DDSs that could be controlled sustainably by external stimuli have been reported, and the drug matrix responded to external stimuli such as light,[13] thermal,[14,15] pH,[16,17] and ultrasound (US)[18,19] to enhance the drug efficiency of DDSs. Such DDS systems in combination with external stimulation have become popular because of their superior drug release efficiency and more precise control of their characteristics.[20,21] Among these stimulants, US retains the advantages of deep penetration, noninvasiveness, and nontoxicity[22] to the human body, as well as simple operation and low cost[21,23] compared to other DDSs. The efficient penetration from the outside to the inside of the body is a major feature not found in other external stimuli and the release of the drug toward the outside of the drug matrix can be controlled by changing the US intensity without loading the specimen.[24,25] In fact, US waves can be transmitted through water and induce oscillatory motion of the surrounding fluid, acoustic streaming, cavitation, and thermal effect.[26,27] US treatment has been proven to be beneficial in a variety of cases,[28] including treatment of diabetes,[29] stroke,[30] cancer,[31] infections,[32] skin dehydration,[33] and bone fractures.[34] On the other hand, we have investigated US-stimulated drug release of biocompatible cellulose hydrogel drugs. In this cellulose hydrogel drug, the water-containing cellulose matrix was hydrogelized by molecular chain entanglement and hydrogen bonding without chemical cross-linking agents; US irradiation cleaved the hydrogen bonding sites, resulting in gel softening, and when the irradiation was stopped, gel regeneration occurred autonomously. Through the US softening effect, the drug release became enhanced toward the opposite side of the drug-hydrogel matrix. In addition to cellulose, a similar effect was observed for chitin, which has a similar chemical structure to CS.[37,38] However, in CS hydrogelized by chemical cross-linkers such as EGDE, there are no reports yet on the sustained drug release of US on this type of hydrogel drug.

In previous research on CS hydrogel drugs, a new semi-interpenetrated (semi-IPN) microsystem using the biocompatible chitosan and poly(ethylene glycol) was developed. Different combinations of these systems were created, loaded with a model drug (methotrexate—MTX), resulting in a faster release of MTX from semi-IPN microspheres in comparison to the pure chitosan microspheres.[35] Curcumin-loaded chitosan/perfluorohexane nanodroplets were used as on-demand drug delivery under sonication, causing the releasing improvement of curcumin.[36] A photo-cross-linkable methacrylated glycol chitosan served as the drug carrier for delivering cells, promoting the survival of cells over an extended period within engineered bioscaffolds.[37] A stabilized porous chitosan composite by glutaraldehyde modulated the immune system and delivered drugs in a controlled manner, facilitating the regeneration of osteochondral reconstruction.[38] A novel catechol-functionalized CS hydrogel linked by genipin was used as the mucoadhesive drug delivery system,[39] by combining chitosan with ethylene glycol acrylate methacrylate via the Michael-addition reaction, resulting in a water-soluble (methacryloyloxy) ethyl carboxyethyl chitosan that was photo-cross-linked. The less harmful effects on cells facilitated their growth effectively, indicating its potential as a promising biomaterial.[40] However, until now, there are few studies on such CS hydrogel loading medicine in the DDS matrix. In US-stimulated drug release, the fundamental process affected drug release, relying on the mechanical or thermal impacts of US.[41] Futhermore, US served as a noninvasive approach to externally stimulated and regulated release of drugs from hydrogels. To enhance delivery effectiveness and reduce potential harm to cells or tissues, especially in upcoming clinical contexts, it is crucial to explore the impacts of US within the delivery system.[42] Against this background, it is significant to examine the US effects of CS/EGDE hydrogel agents and those of covalent cross-linked gel properties, which are different from cellulose and chitin hydrogel agents, as in the original report. Hence, it is important to fully characterize CS/EGDE hydrogel drugs when adapting US external triggering to drug release. In the present study, US-triggered DDSs based on amoxicillin-loaded CS/EGDE hydrogel are described. Here, the drug amoxicillin (Amox) is an analog of ampicillin, has a semisynthetic antibiotic effect, and is used to treat bacterial infections for wound-healing treatment because it has essentially the same broad spectrum of bacteriocidal activities against many Gram-positive and certain Gram-negative microorganisms.[43] Thus, the drawbacks of antibiotics, such as overdosage, toxicity, and stability, can be controlled with the use of Amox-entrapped hydrogels. As a potential drug release technique, we aim to investigate the Amox-entrapped hydrogel of the CS/EDGE matrix and US-stimulated amoxicillin release. For the purpose of studying the CS/EGDE hydrogel properties of US, the effect of US on the Amox-entrapped hydrogel drugs is investigated.

2. EXPERIMENTAL SECTION

2.1. Materials. Chitosan (degree of deacetylation = 80%) was supplied from (KATOKICHI CO., LTD, Japan), and ethylene glycol diglydicyl ether (EGDE) and amoxicillin trihydrate were provided by TCI Chemicals Co., Ltd., Japan. Other chemicals were analytical grade and used without further purification.

2.2. Fabrication of Amox-Entrapped Chitosan/EGDE Hydrogel Drug. In CS-EGDE hydrogelation from their aqueous solutions, the chitosan concentrations ranged from 1 to 3% in 3% acetic acid aqueous solution (Scheme 1). Here, the sample names were 1% CS/EGDE, 1.5% CS/EGDE, 2% CS/EGDE, 2.5% CS/EGDE, and 3% CS/EGDE for 1, 1.5, 2, 2.5, and 3% of CS concentration, respectively. Then, the cross-linker agent of EGDE was added dropwise under constant stirring to chitosan solution with an equivalent amount of EGDE to CS for 24 h before placing in 3.5 cm-diameter Petri dishes. Next, the CS/EGDE solution was left at room temperature and gelled into a solid-like substance in 1 M NaOH for 12 h. The gelatinous solid forms were extensively rinsed with DI water until neutrality to eliminate NaOH and were then stored in DI water before testing. The introduction of the drug Amox into the gelatinous matrix was performed by immersing the CS/EGDE hydrogel in the 0.1% aqueous Amox solution for 24 h at room temperature. Then, to remove the Amox unbonded, the hydrogel drugs were carefully washed by 30 mL of DI water 3 times.

2.3. Characterization of Amox-Entrapped CS/EGDE Hydrogel Drugs. To investigate the gelation behavior of CS/EGDE alkaline aqueous solutions, the time variation of

https://doi.org/10.1021/acsomega.3c06213
ACS Omega 2024, 9, 585−597

Scheme 1. Process to Synthesize CS/EGDE/Amox Hydrogels

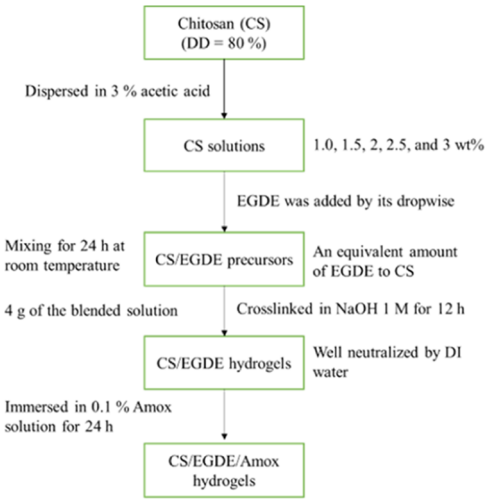

dynamic viscoelasticity, storage modulus G', and loss modulus G'' were tracked at room temperature by a rheometer (Physica MCR 301, Anton Paar, Austria). The measurement was applied for a time-sweep oscillation at 1 Hz and 1% strain for 2000 s for time change in G' and G'', when the strain % was in the range of 0.1−1000%, while tan = G''/G' values were also recorded at each strain rate to determine the viscoelasticity of the CS/EGDE/Amox hydrogel with and without US exposure for 2 h. The water content (WC) of the prepared hydrogels was calculated using the formula 1

$$\mathrm{WC} = (W_0 - W_1)/W_1 \times 100\% \quad (1)$$

where W_0 and W_1 represent the hydrogel in wet and dry states, respectively. Before measuring the value of W_0, the hydrogel surface was gently cleaned and the matrices were evacuated in a vacuum dryer at 50 °C for 24 h for complete drying. Using a multifunction balance (GX-200, A&D Company Limited, Japan), the density of Amox-entrapped CS/EGDE hydrogels was determined at 25 °C with three samples.

The Amox amounts entrapped in the hydrogels were determined according to a previous technique with a few modifications.[44] To do this successfully, the Amox-entrapped hydrogel was sliced into small pieces and placed into 15 mL of distilled water under stirring for 2, 24, and 48 h at room temperature, allowing the entrapped Amox to escape into the aqueous medium. The experiment was repeated separately for three specimens to ensure repeatability.

In the Amox releasing experiments, the release of Amox from the Amox-entrapped CS/EGDE hydrogel was measured in a US water bath as depicted in Figure 3b. The hydrogel matrix (d = 25 mm, h = 3 mm) was placed in a sample holder with 30 mL of phosphate buffer solution (PBS) at pH 7.4. In a sonoreactor device, the US water bath (φ 86 mm × 65 mm) was equipped with a Langevin-type transducer (HEC-45242M, Honda electrics Co. Ltd., Japan) at a temperature of 25 °C. Using a wave factory (WF1943B multifunction synthesizer, NF, Japan), the US power output was set in the range from 0 to 35 W. Amox released in the PBS solution of the US water bath was detected by quantifying the intensity of the absorption peak at 273 nm (JASCO V-570 UV/vis/NIR spectrophotometer). Also, as shown in Figure 3a, to measure the ultraviolet−visible (UV−vis) spectra of the Amox-entrapped CS/EGDE hydrogel and CS/EGDE hydrogel, samples were sliced with about 1.48 mm thickness and sandwiched between quartz plates. To explore the drug release mechanism from the hydrogel or for more than one sort of release phenomenon, the mathematical models were utilized to determine the drug release kinetics from the CS/EGDE/Amox hydrogel network according to previous reports[45,46]

$$\text{zero order: } C_t/C_0 = k_0 t \quad (2)$$

$$\text{first order: } \log C_t/C_0 = -k_1 t/2.303 \quad (3)$$

$$\text{Higuchi: } C_t/C_0 = k_h t^{0.5} \quad (4)$$

$$\text{Korsmeyer} - \text{Peppas: } \log(C_t/C_0) = \log(k) + n\log(t) \quad (5)$$

$$\text{Hixson} - \text{Crowell: } C_o^{1/3} - C_t^{1/3} = k_{hc} t \quad (6)$$

where C_t denotes the quantity of drug released at time t and C_0 is the initial concentration of the drug in the hydrogel. The release rate constants for zero order, first order, Higuchi model, Korsmeyer−Peppas model, and Hixson−Crowell

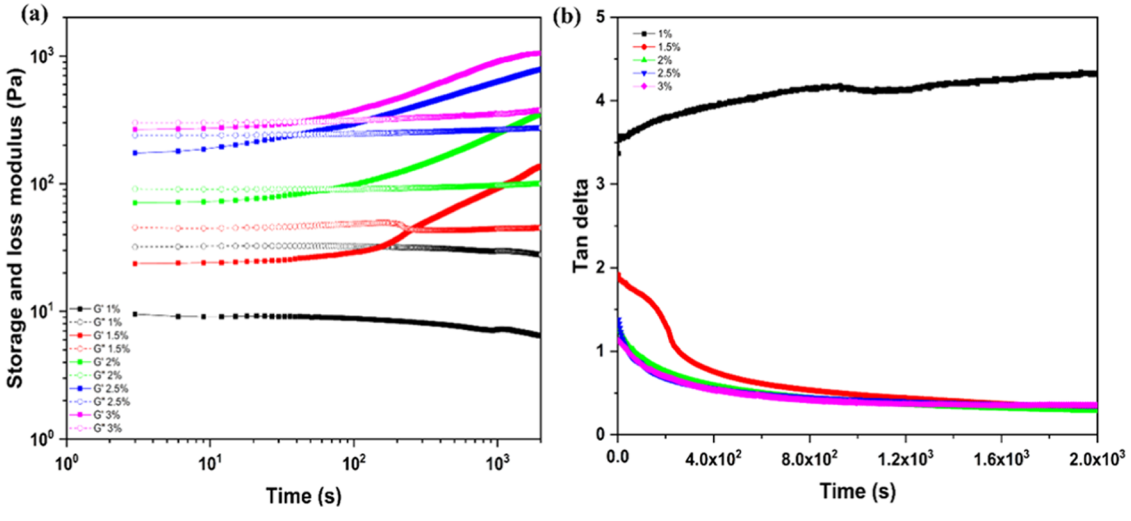

Figure 1. (a) Time change of G' and G'' and (b) tan δ for the CS/EGDE solutions with various CS concentrations.

https://doi.org/10.1021/acsomega.3c06213
ACS Omega 2024, 9, 585−597

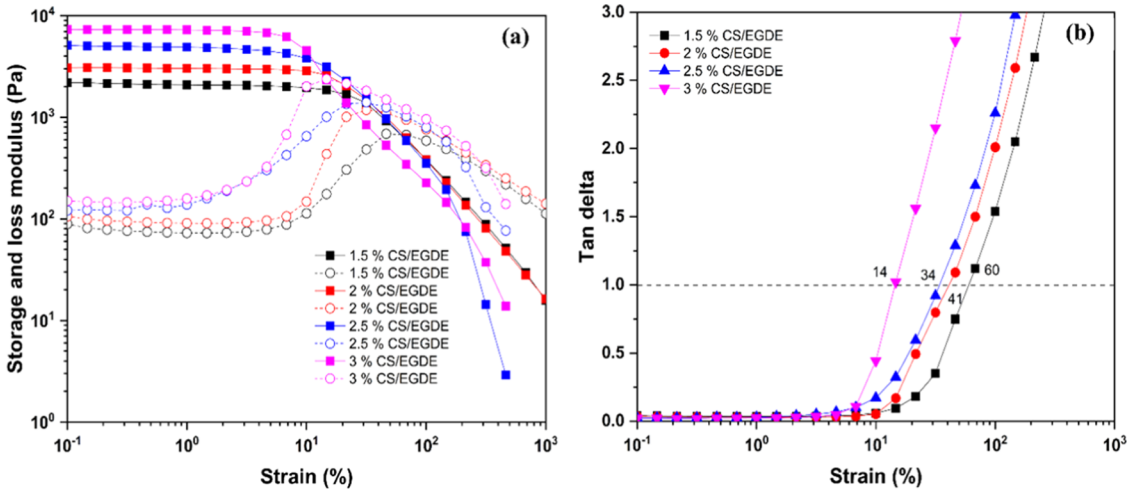

Figure 2. (a) G' and G'' and (b) tan δ at different strain % for the CS/EGDS hydrogels. These hydrogels were washed with large volumes of water and tested on samples with a pH of 7 in the water they contain.

Table 1. Properties of the CS/EGDE and CS/EGDE/Amox Hydrogels

					water content (%) dry basis	
samples	gelation time (s)	G' at 0.1% strain (Pa)	Amox-encapsulated amount (μg/g hydrogel)	density (g/cm^3)	before US exposure	after US exposure
1.5%CS/EGDE	254	2210		0.936 ± 0.004	2929 ± 24	
2%CS/EGDE	70	3100		0.940 ± 0.003	2480 ± 26	
2.5%CS/EGDE	40	5010		0.941 ± 0.003	2134 ± 17	
3%CS/EGDE	40	7310		0.950 ± 0.002	1814 ± 21	
1.5%CS/EGDE/Amox		2200	188 ± 16	0.939 ± 0.006	3010 ± 38	3149 ± 42
2%CS/EGDE/Amox		2950	252 ± 28	0.944 ± 0.001	2600 ± 58	2686 ± 25
2.5%CS/EGDE/Amox		3950	211 ± 22	0.945 ± 0.003	2268 ± 24	2261 ± 35
3%CS/EGDE/Amox		5520	208 ± 14	0.952 ± 0.000	1984 ± 27	1957 ± 30

model are k_0, k_1, k_h, k_{hc}, and k, respectively, and n is the release exponent, which indicates the release mechanism for the Korsmeyer−Peppas model.

The viscoelastic behavior of Amox-entrapped CS/EGDE hydrogels was measured by Auto Paar-Reoplus equipment (Auton Paar Japan, Tokyo) with a constant frequency of 1 Hz at room temperature. For the US-triggered hydrogels, the amplitude sweep was measured before and after US exposure for 120 min. The relationship between storage modulus G' and loss modulus G'' and strain in the range of 0.1−1000% was recorded.

The Fourier-transform infrared (FTIR) spectra of the Amox-entrapped CS/EGDE hydrogels were analyzed using the FTIR spectra of a JASCO FT/IR-4100 (JASCO Corporation, Japan) in the 4000−500 cm^{-1} range with a resolution of 4 cm^{-1} and an average of 16 scans. The scanning electron microscope (SEM) JSM-5300 LV (JEOL, Japan) was used for observation of hydrogel morphology. The Amox-entrapped CS/EGDE hydrogels were frozen in liquid nitrogen and then water was eliminated from the frozen matrix followed by freeze-drying. To confirm the dispersion of Amox in the hydrogel matrix, the cross sections was observed using an energy-dispersive spectrometer (EDS). After sputtering gold using a fast cool coater (Sanyu Denshi K.K., Japan), the cross sections of hydrogel samples were inspected and photographed.

3. RESULTS AND DISCUSSION

3.1. Gelation Behavior of Aqueous CS/EGDE and Viscoelasticity of the Resultant CS/EGDE Hydrogels.

Using dynamic viscoelasticity analysis, the gelation of CS/EGDE solutions was investigated for different concentrations of 1, 1.5, 2, 2.5, and 3% CS. Figure 1a depicts the time change of G' and G'' moduli in the concentration range of 1−3%. For viscoelastic measurements, the strain% was 1 Hz and mechanical oscillation was 1%. As the CS concentrations rose from 1 to 3% of the CS/EGDE solution, the values of G' tended to increase with increasing time. In addition, both G' and G'' values increased at time zero with increasing concentration. This is due to the higher viscosity of the CS/EGDE solution at higher concentrations. However, at 1% CS concentration, the G' to G'' values were almost constant with respect to time. In this case, gelation by cross-linking reaction did not occur within this time. In contrast to this, especially at concentrations of 1.5, 2, 2.5, and 3%, G' started to increase at about 200, 30, 11 and 10s, respectively. These results indicate that gelation of CS/SGDE solutions tends to shorten with increasing CS concentration. During the gelling processes, for example, the G' value increased from 25 Pa at 30 s to 10^2 Pa at 2000 s for the 1.5% CS/EGDE solution. This trend became clearer with time variation of tan δ, the ratio of G'' to G' (Figure 1b). Namely, the value of tan δ declined precipitously at a particular time and then became constant. At the moment when tan δ = 1, the aqueous CS/EGDE solution solidified as a result of liquefaction. The decrease trend in the gelation time was seen from 254, 70, and 40 s for 1.5, 2, and 3% CS concentrations, respectively, meaning that gelation occurred faster at higher CS concentrations. However, even with tan δ = 1 and in the solidified state, the value continued to decrease

https://doi.org/10.1021/acsomega.3c06213
ACS Omega 2024, 9, 585−597

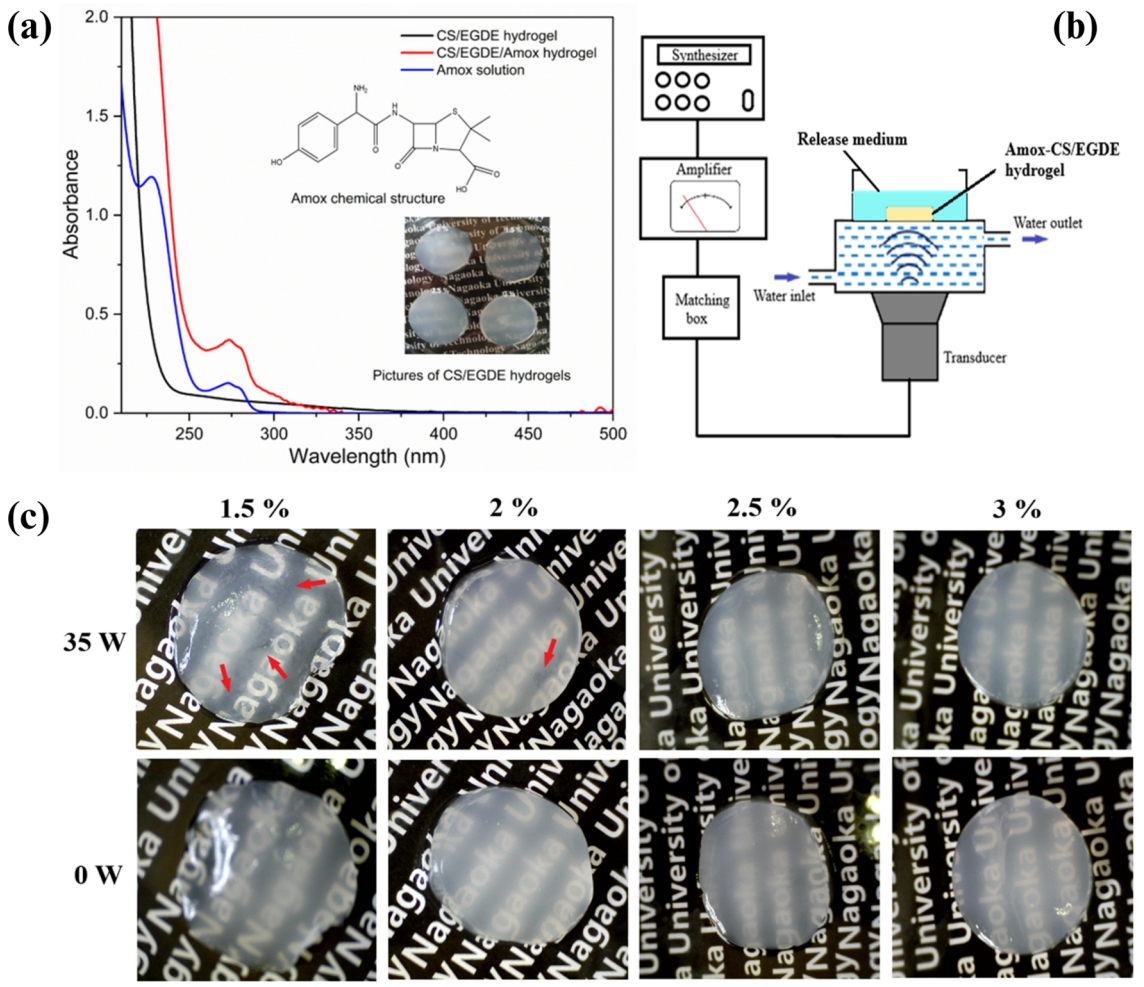

Figure 3. (a) UV−vis spectra of the CS/EGDE hydrogel and CS/EGDE/Amox hydrogel with 1.37 and 1.48 mm thickness, respectively, and Amox aqueous solution at 50 μg/mL, Amox chemical structure, and external appearance of CS/EGDE hydrogels without Amox; (b) US experimental setup; and (c) appearance picture of CS/EGDE/Amox hydrogels prepared with different CS percentages in the absence and presence of US-triggered release at 35 W.

after this time passed, indicating that gelation was in progress until the time when the value of tan δ became constant. At higher concentrations of CS, the value remained almost the same for about 800 s. When the concentration decreased to 1.5% CS, the value was 1600 s, and at 2% CS, it was about 1000 s.

Figure 2a shows the relationship between G', G'', and strain % and Figure 2b shows the tan δ at each strain % for the CS/EGDE hydrogels. The value of G' at 0.1% strain was larger for hydrogels with higher CS concentration, for example, 7.3×10^3 Pa at 3% CS/EGDE and 2.2×10^3 Pa at 1.5% CS/EGDE, indicating that increasing concentration tended to make the gel harder. In the relationship between tan δ and strain, the strain % at tan δ = 1 was 60% for the softer 1.5% CS/EGDE, while for the harder 3% CS/EGDE, strain % = 14%. Thus, the harder CS/EGDE hydrogels showed less deformation-induced collapse of the gel structure compared to the softer ones.

The properties of these hydrogels when entrapped with Amox are compared to those of CS/EGDE without Amox in Table 1.The soft 1.5% CS/EGDE hydrogel showed less density than the hard 3% CS/EGDE hydrogel in the Amox-free CS/EGDE before the drug was entrapped. Conversely, the water content was 2929 ± 24% for the former, indicating more water retention than the latter 3% CS/EGDE having 1814 ± 21%. As seen in Figure 3a, Amox has an absorption peak at 273 nm assigned for the $\pi-\pi^*$ transition. In the 2% CS/EGDE hydrogel, the band was detected, indicating the presence of Amox with an aromatic ring with $\pi-\pi^*$ transition. The presence of the peak at 273 nm in the CS/EGDE/Amox hydrogel demonstrated the incorporation of Amox in the hydrogel. To study US-triggered Amox release activity from CS/EGDE/Amox hydrogels, the manufactured hydrogel was subjected to US using the experimental setup illustrated in Figure 3b. The hydrogels were placed in a US water tank and 43 kHz US was exposed from the bottom. In the water bath, the Amox triggered by US and released from the CS/EGDE/Amox hydrogel was estimated by absorbance change at 273 nm.

As seen in Figure 3c, the appearance pictures of Amox-entrapped CS/EGDE hydrogels in the presence and absence of US almost resembled the Amox-free one that retained a great deal of water. Table 1 shows that the water content of the Amox-free hydrogels ranged from about 1800 to 3000%; the water content of those CS/EGDE/Amox hydrogels was somewhat increased after Amox absorbed inside the gel matrix by immersing these hydrogels in 0.1% Amox solution for 24 h. However, after the 35 W US was applied for 120 min, the water contents of hydrogels irradiated with 1.5% CS/EGDE/

https://doi.org/10.1021/acsomega.3c06213
ACS Omega 2024, 9, 585−597

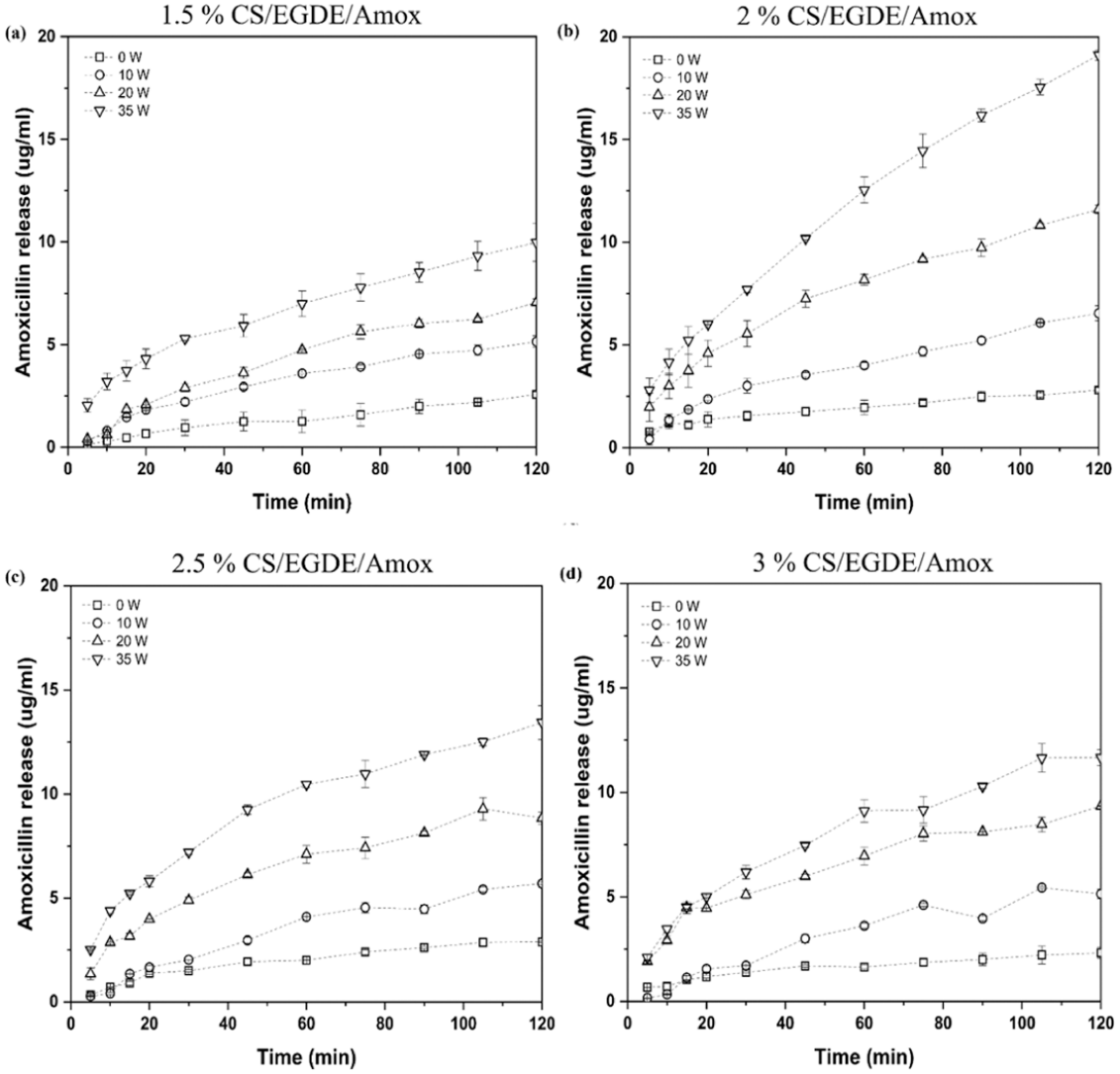

Figure 4. Concentration of Amox released into aqueous PBS solution; pH 7.4 was measured against ultrasonic (US) exposure time. The US irradiation was conducted with a frequency of 43 kHz, power of 0−35 W, and temperature of 25 °C at various CS contents with 1.5% (a), 2% (b), 2.5% (c), and 3% (d).

Amox, 2% CS/EGDE/Amox, 2.5% CS/EGDE/Amox, and 3% CS/EGDE/Amox were 3149 ± 42, 2686 ± 25, 2261 ± 35, and 1957 ± 30%, respectively. A comparison of the water content in Table 1 and postultrasonic irradiation values showed a slight increase in water retention with US irradiation. A similar trend was observed for cellulose hydrogels[44] and chitin hydrogels.[25] This trend was evident for the flexible 1.5 and 2% CS/EGDE/Amox, but not for the rigid hydrogel, 3% CS/EGDE/Amox; on the contrary, the moisture content decreased. This might be due to the dehydration of amino groups that were hydrogen bonded to the water in the dense chitosan environment to the outside of the hydrogel by US irradiation.

Figure 6a shows the SEM images of Amox-loaded 1.5% CS/EGDE, 2% CS/EGDE, and 3% CS/EGDE. The inner structure of these hydrogels, magnified by 1000× and 5000×, showed a sponge network of CS, forming a dense structure as the CS concentration increased from 1.5 to 3%. This difference in structure at 5000× is thought to be the reason that the 3% CS/EGDE with its dense CS mesh structure had a reduced water content because the hydrogel that absorbed the water did not have enough space to hold the water. However, in 1.5% CS/EGDE, there was enough space to hold water, and it could be inferred that swelling was facilitated. Also, as shown on the right, the EDS patterns of sulfur S and carbon C were exhibited as red and blue dots. The Amox-derived S was found to be widely distributed within the inner sponge structure of the gel after immersion of each hydrogel in the Amox solution.

3.2. US-Stimulated Amox Release from CS/EGDE/Amox Hydrogels. Figure 4 shows the time course of Amox releasing amounts under US exposure with 0, 10, 20, and 35 W for (a) 1.5% CS/EGDE/Amox, (b) 2% CS/EGDE/Amox, (c) 2.5% CS/EGDE/Amox, and (d) 3% CS/EGDE/Amox hydrogels. The comparison was enabled for the Amox release without and with US by varying the output powers of 10, 20, and 35 W at 43 kHz. It was observed that the released amount of Amox increased with increase of the time, even though US was not irradiated as seen in 0 W. All samples in the US system had a higher release than the results without US. In addition, with increasing US power from 10 to 35 W, the Amox release amounts became high when the exposure time increased. Among those Amox-entrapped hydrogels, the highest sustained release of Amox was observed with 2% CS/EGDE/Amox. The

https://doi.org/10.1021/acsomega.3c06213
ACS Omega 2024, 9, 585−597

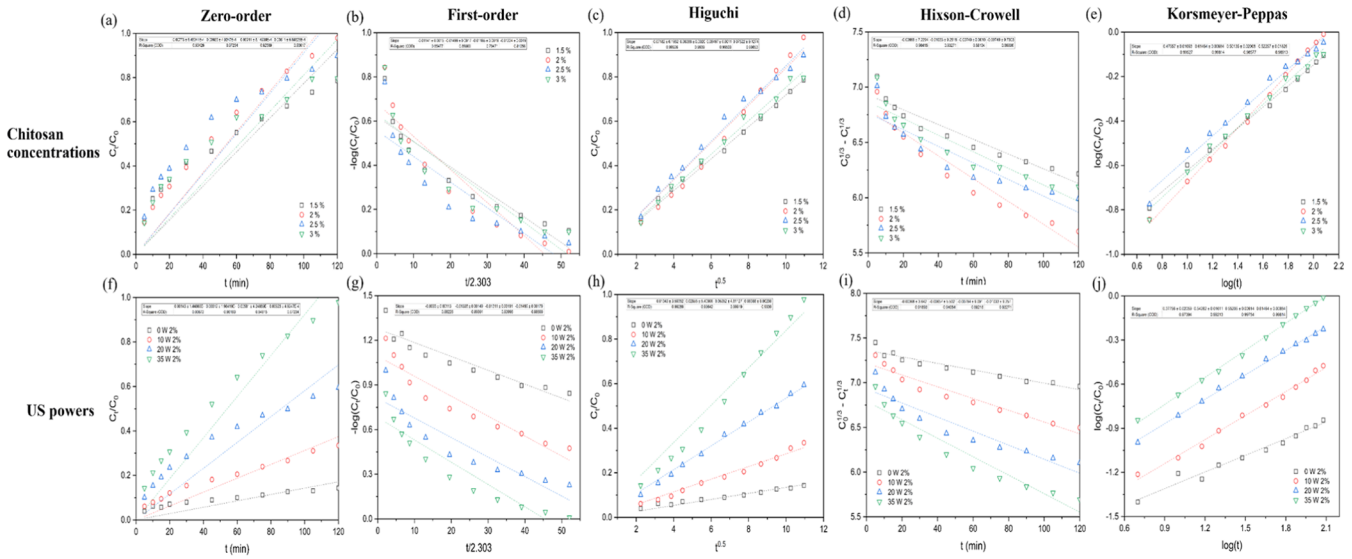

Figure 5. Kinetic models of Amox release profile from CS/EGDE/Amox hydrogels: (a, f) zero order, (b, g) first order, (c, h) Higuchi model, (d, i) Hixson-Crowell model, and (e, j) Korsmeyer-Peppas model of 1.5, 2, 2.5, and 3% at 35 W/43 kHz; 0, 10, 20, and 35 W of 2% CS/EGDE/Amox, respectively.

quantity reached roughly 19 μg/mL at 35 W for 120 min, 10 μg/mL at 20 W, and 5 μg/mL at 10 W. In contrast, the sustained release of 1.5, 2.5, and 3% CS/EGDE/Amox was lower than that of 2% CS/EGDE/Amox. Similar results were observed for cellulose hydrogels:[44] the initial drug contents inside the hydrogels influenced the quantity of drug amounts released when US exposure was operated. In the case of 2% CS/EGDE/Amox, the entrapped Amox was 252 ± 28 μg/g hydrogel. However, the quantity of Amox entrapped in the 1.5% CS/EGDE/Amox hydrogels was 188 ± 16 μg/g hydrogel, and for 3% CS/EGDE/Amox it was 208 ± 14 μg/g hydrogel; the variation in the trapped Amox quantities observed in the hydrogels formed with different CS concentrations can be attributed to the density of CS, as shown in Table 1. Therefore, it was understood that in the case of 1.5% CS/EGDE/Amox, where the amount of drug in the gel matrix was small, the amount of sustained release was also reduced. 3% CS/EGDE/Amox also showed less Amox loading than 2% CS/EGDE/Amox, but more than 1.5% CS/EGDE/Amox. The Amox density and cross-link density were responsible for the variations in entrapped Amox levels in the hydrogels, as Amox was entrapped through the process of immersion of the hydrogel matrix in an aqueous Amox solution. The reason is that a high porosity with intermediate matrix density was produced at 2% CS/EGDE, providing more space for Amox loading in the CS/EGDE network. According to the SEM images in Figure 6b, the hydrogel matrix of 2% CS/EGDE in the presence of US was loosened and roughed. Futhermore, the morphology of 2% CS/EGDE/Amox was somewhat shrunk and roughed by US irradiation because the hydrogel pores were influenced by the external US power, causing the collapse of the porous structure after releasing Amox under US exposure. As a result, after 120 min release, a considerable reduction of Amox from the 2% CS hydrogel matrix was seen at 35 W US exposure, while in the case of natural release without US stimuli, the red color points still remained as shown in the EDS pictures. That result made sense with drug release data; Amox could release more effectiveness under US response.

To better understand the drug release behavior of the hydrogel, mathematical models including zero order, first order, and Hixson−Crowell, Higuchi, and Korsmeyer−Peppas models were fitted to the data of Figure 5. The physical parameters obtained for the release exponent (n) and correlation coefficient (r^2) are tabulated in Table 2. Upon analysis, it was found that it adhered to both the Higuchi and Korsmeyer-Peppas models assuming that Amox release from the hydrogel matrix entrapped with the drug occurred via diffusion. Thus, it was suggested that the effect of US had the potential to enhance the diffusion of Amox from within the gel matrix to the outside. Besides this, the rate of drug release is proportional to the square root of time.[47] Korsmeyer−Peppas model assumed that drug release occurred by a combination of diffusion-controlled and relaxation-controlled systems.[48] It was noticed in the kinetic results shown in Table 2. Amox release followed a non-Fickian distribution with n values ranging from 0.45 to 0.70 for the CS/EGDE/Amox hydrogels, when US was operated at 35 W/43 kHz, and the r^2 value for all conditions was greater than 0.95, meaning well fitting. However, in the case of changing US powers from 10 to 35 W of the 2% CS/EGDE/Amox sample, the results of n values were 0.54, 0.55, and 0.61, respectively. Thus, drug release occurs as a consequence of both diffusion and relaxation of the porous hydrogel matrix. However, the n-value of the 2% CS hydrogel in the absence of US was 0.38, lower than 0.45, indicating that Amox release from this hydrogel followed the Fickian process, meaning Amox release by diffusion only.

3.3. US Influence on CS/EGDE/Amox Hydrogels Matrix. As is widely known, viscoelasticity information is helpful for evaluation of the gelatinous properties of polymeric hydrogels.[49] Figure 7a,c,e,g depict the G' and G'' values of those CS/EGDE/Amox hydrogels before and after US irradiation for 120 min. Comparison of the G' values in Table 1 between CS/EGDE and CS/EGDE/Amox showed that the G' values at 0.1% strain tended to decrease when Amox was entrapped. But it was evidently apparent that the G' value at 0.1% strain increased when the hydrogels were varied from 1.5% CS/EGDE/Amox to 3% CS/EGDE/Amox. The

https://doi.org/10.1021/acsomega.3c06213
ACS Omega 2024, 9, 585−597

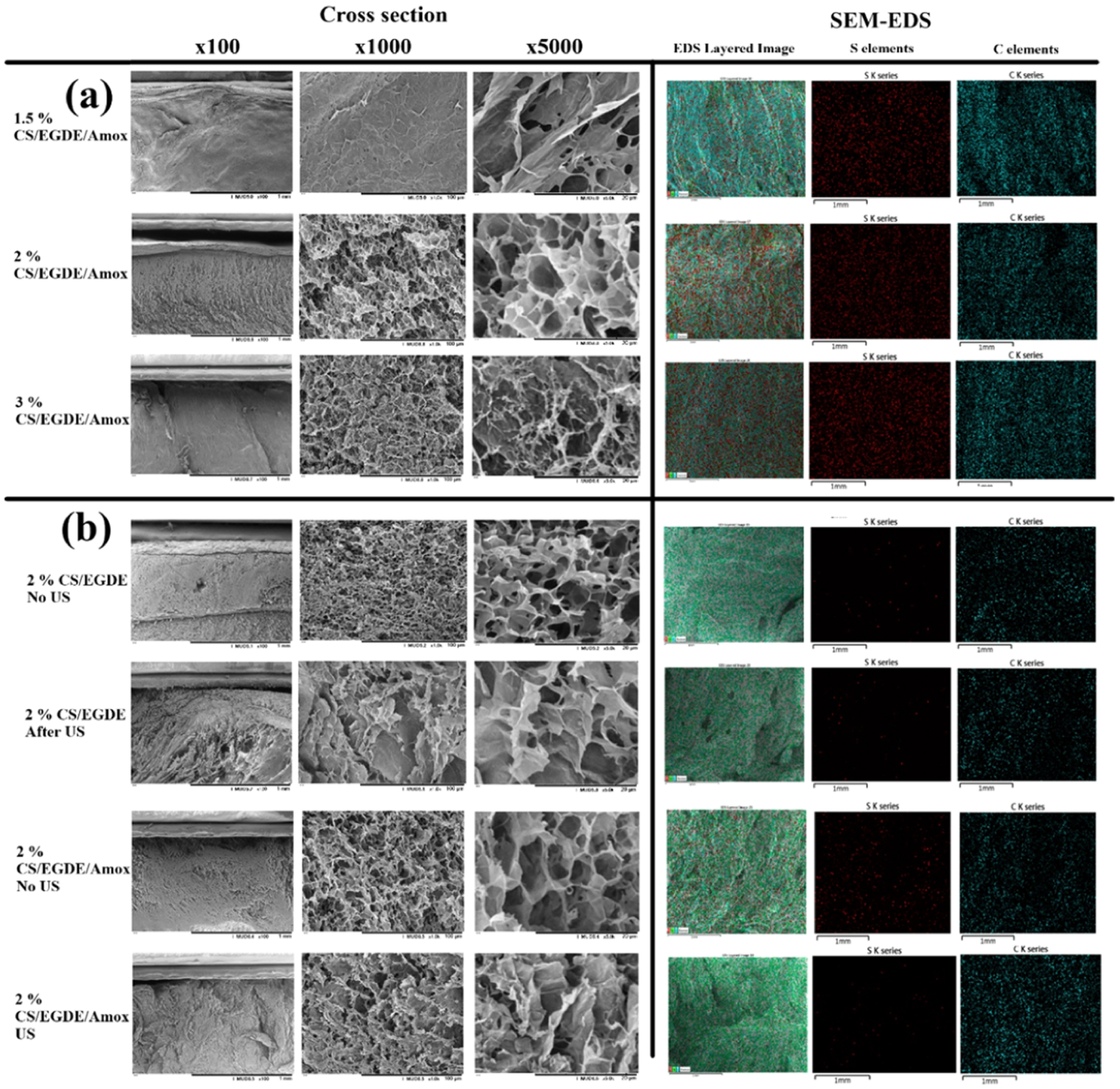

Figure 6. Cross-sectional SEM images of the Amox-entrapped CS/EGDE hydrogels before releasing (a); 2% CS/EGDE hydrogels and 2% CS/EGDE/Amox hydrogels after releasing Amox in the absence and presence of US for 120 min (b) in 100×, 1000×, and 5000× magnification (left); EDS layered photo and S and C elements of those hydrogels (right).

decrease in G' due to Amox entrapping appears to be due to Amox incorporation through interaction with amino groups. However, the increase in G' with increasing CS concentration from 1.5 to 3% could be attributed to the dense gel network in addition to the increase in density. In the FTIR spectra as shown in Figure 8, the absorption bands of the Amox-derived C═O group were seen at 1750 cm^{-1} and O−C−O at 1240 cm^{-1}, indicating that Amox was definitely in the 2% CS/EGDE/Amox hydrogel. Here, the Amox spectrum had such characteristic bands at 1759 and 1241 cm^{-1}. So the comparison between Amox and CS/EGDE/Amox indicated the C═O band peak appeared in the CS/EGDE/Amox shifted toward the low wavenumber side, resulting in interaction of the Amox entrapped with CS. A similar thing could be seen with C═O band peaks in the spectra of the 2% CS/EGDE/Amox before and after water washing after immersion in Amox aqueous solution. Namely, even with water washing, the observed Amox band was retained in the hydrogel due to its interaction with CS. The peak observed at 3330 cm^{-1} in the CS corresponded to the vibrational stretching overlapping peaks of N−H and O−H intermolecular and intramolecular hydrogen bonds. Apparently, the overlapping peak top became broadened compared with that of the CS/EGDE, which had no Amox. The stretching vibrational absorption peak of C−H along the CS chain was detected at approximately 2879 cm^{-1}. Furthermore, the absorption peaks of CS were identified at 1645 (amide I), 1567 (amide II), and 1387 cm^{-1} (amide III), which can be attributed primarily to the stretching vibration of

https://doi.org/10.1021/acsomega.3c06213
ACS Omega 2024, 9, 585−597

Table 2. Kinetic Models of Amox-Loaded CS/EGDE Hydrogels: Diffusion Exponents, Diffusion Types, and Regression Values in PBS 2 mM, pH 7.4

		kinetic models					
		zero order	first order	Higuchi	Hixson–Crowell	Korsmeyer–Peppas	
parameters		r^2	r^2	r^2	r^2	n	r^2
Chitosan concentration (%) at 35 W, 43 kHz	1.5	0.934	0.855	0.999	0.904	0.48	0.995
	2	0.972	0.887	0.994	0.933	0.61	0.998
	2.5	0.926	0.795	0.998	0.851	0.50	0.986
	3	0.936	0.811	0.998	0.868	0.52	0.989
US powers (W) for 2% CS/EGDE/Amox	0	0.907	0.882	0.993	0.919	0.38	0.974
	10	0.962	0.899	0.996	0.941	0.54	0.992
	20	0.949	0.840	0.999	0.892	0.55	0.998
	35	0.972	0.887	0.994	0.933	0.61	0.998

C–O, the vibration of the N–H bond, and the stretching vibration of the C–N bond, respectively, and the peaks of 2% CS/EGDE/Amox appeared at 1750, 1387, and 1215 cm^{-1}. Even though the peaks of Amox-entrapped CS/EGDE slightly shift as compared with Amox spectra, this meant CS-Amox interaction. Two peaks were observed at 1141 and 1021 cm^{-1} for the characteristic saccharide backbone corresponding to the antisymmetric stretching of the C–O–C bridge and the C–O vibration of the ring. Figure 8 also shows the spectrum measured after US irradiation at 35 W for 120 min. In this spectrum, the characteristic C=O of Amox almost disappeared, suggesting that its sustained release had almost taken place. The spectrum of the remaining hydrogel was almost the same as that before the entrapment of Amox. This suggested that no decomposition of the hydrogel occurred even after 120 min of sonication.

Figure 7 shows the change of G' and G'' at strain% when each CS/EGDE hydrogel was irradiated with 35 W US. For 1.5% CS/EGDE/Amox, 2% CS/EGDE/Amox, 2.5% CS/EGDE/Amox, and 3% CS/EGDE/Amox, respectively, the G' value remained almost constant at 2200, 2950, 3950, and 5520 Pa, respectively. Furthermore, as strain% was increased, the G' decreased, indicating that the hydrogel structure collapsed and liquefied with increasing the strain. The values of G'' were constant up to about 10% strain for all hydrogels, but gradually increased and approached the value of G'. When $G' = G''$, at the strain %, transition from solid gel to liquid gel occurred. So the values at $\tan\delta = 1$ were 100, 99, and 71% strain for 1.5% CS/EGDE/Amox, 2% CS/EGDE/Amox, and 3% CS/EGDE/Amox at 0 W, respectively. Therefore, the harder hydrogel of 3% CS/EGDE/Amox tended to produce a lower strain % of gel structure collapse due to mechanical stress than the softer one of 1.5% CS/EGDE/Amox. This might be because a harder hydrogel cannot well absorb the mechanical shear force provided by the rheometer. The results of the same measurements with 35 W US irradiation showed almost the same strain % change as the unirradiated 0 W results; for 2% CS/EGDE/Amox, US intensities of 10 and 20 W were also shown with the 35 W results. However, as the US intensity increased, the G' values in 0.1–30% strain range decreased. Also, the strain % at $G' = G''$ changed from around 127% to about 90% as the US intensity increased in the case of 2% CS/EGDE/Amox. This result indicated that, in addition to mechanical deformation, US shear forces deformed the hydrogels and accelerated the collapse of the gel structure when US was applied. Therefore, the decrease in G' upon US irradiation was considered to be caused by the US-induced collapse of the hydrogel under mechanical strain. Ebaborately, the influence of different US powers on the G' value at 0.1% strain of 1.5, 2, 2.5, and 3% CS/EGDE/Amox hydrogels are plotted in Figure 7i. The G' values trended downward when the US output power was enhanced from 0 to 35 W for 1.5 and 2% CS/EGDE/Amox due to the softening effect of US. For 2% CS/EGDE/Amox hydrogel, the G' value at 0.1% strain at 0, 10, 20, and 30 W were 2950 2680, 2010, and 1800 Pa, respectively. This meant that when the US power increased, the gel became softened by gel structure deformation and the considerable amount of Amox release from hydrogels during US irradiation causing the decrease in the G' value. Furthermore, the stimulatory effect of US on the hydrogel matrix was observed, regardless of the variations in chitosan concentrations among these hydrogel systems. The reduction trend of G' value was not significant as seen for higher CS contents at 2.5 and 3% CS/EGDE/Amox because the US force might not effective in the case of a dense covalent cross-linking network.

There were prior examples of viscoelastic changes in hydrogels upon US irradiation in cellulose hydrogels,[50] in which the mechanical shear force of the rheometer combined with the shear force of US resulted in a higher degree of change than that of CS/EGDE hydrogels. The change of strain % at $G' = G''$ was also greater for the cellulose hydrogels.[44,51] In the case of cellulose hydrogels, gelation was mainly due to hydrogen bonding and entanglement of the molecular chains, but no covalent cross-linking like CS/EGDE. In the cellulose hydrogel, hydrogen bond disruption contributed to the softening of the gel due to a decrease in viscoelasticity. In contrast, in the case of CS/EGDE, gelation is due to the covalent bonding between CS and EGDE, so US softening of the gel was unlikely to occur because the covalent bonds are stronger than the hydrogen bonds. As a result, the enhanced sustained release of Amox from the CS/EGDE hydrogels might have contributed to the enhanced diffusion and relaxation of the hydrogel matrix suggested by the kinetics analysis, rather than the disintegration of the gel matrix by ultrasonic shear forces.

4. CONCLUSIONS

In the present study, the release of Amox from the CS/EGDE/Amox hydrogel matrix in response to US was studied under various US powers (0–35 W) at 43 kHz. When the CS concentrations for gelation were increased, the resultant hydrogel matrices formed a dense CS network, especially in 3 wt %. In the case of the Amox-entrapped CS/EGDE hydrogel, 2% CS/EGDE could entrap a greater amount of

https://doi.org/10.1021/acsomega.3c06213
ACS Omega 2024, 9, 585–597

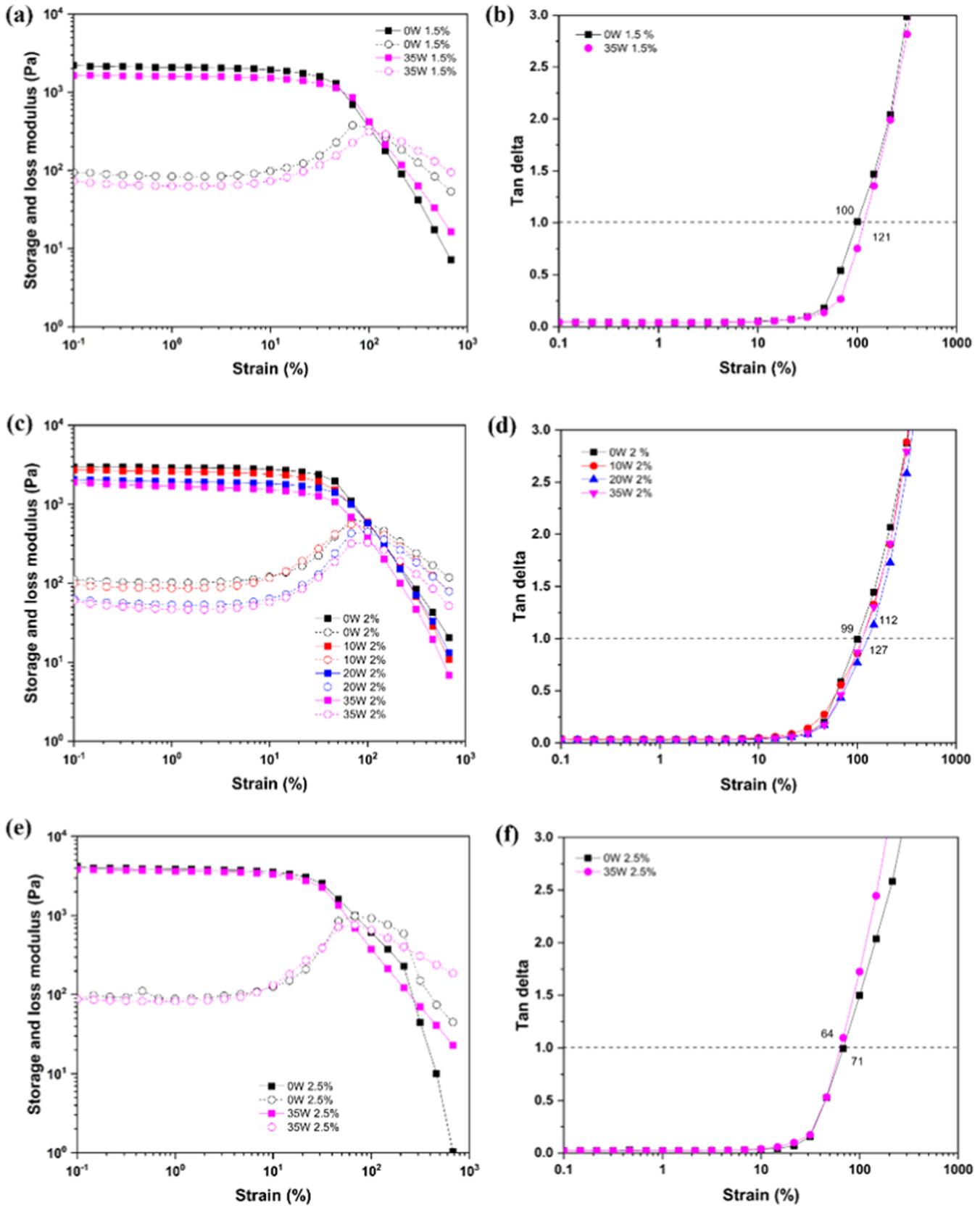

Figure 7. Amox-trapped CS/EGDE hydrogels were subjected to strain sweep measurements (a−g) with corresponding tan δ measurements (b−h), both with and without ultrasonic exposure (43 kHz, 35 W, 120 min). These hydrogels were made from CS solutions with concentrations of 1.5 wt % (a, b), 2 wt % (c, d), 2.5 wt % (e, f), and 3 wt % (g, h). The measurements were performed at a frequency of 1 Hz and characterized by G' (storage moduli), G'' (loss moduli), and tan δ, which is defined as the ratio of G'' to G'. The relation between G' at 0.1% strain of Amox-CS/EGDE hydrogels at 1.5 to 3% of CS and US powers at 0, 10, 20, and 35 W (i).

https://doi.org/10.1021/acsomega.3c06213
ACS Omega 2024, 9, 585−597

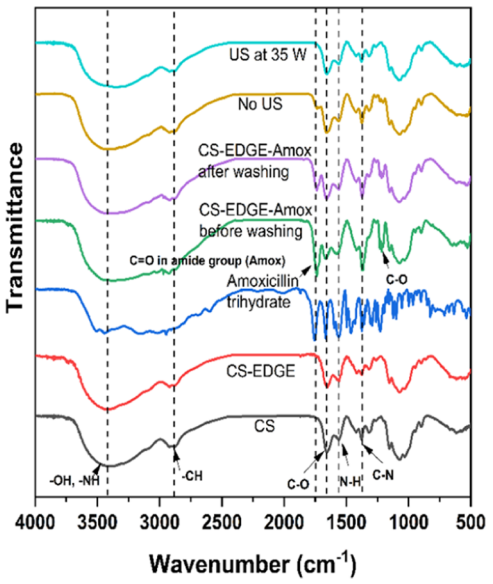

Figure 8. Chemical structure confirmation of CS/EGDE hydrogels and Amox-loaded CS/EGDE hydrogels before and after release with/without US exposure.

Amox entrapment due to its porous structure, resulting in efficient Amox release under US triggering. As the US power increased from 10 to 35 W at 43 kHz, the release efficiency of the drug also increased. The drug release data of the hydrogels were fitted with the Higuchi model and Korsmeyer-Peppas model, emphasizing the sustained release behavior of the hydrogels with a non-Fickian diffusion mechanism under US stimuli. This meant the mechanism was a combination of diffusion and relaxation of polymer in DDS. However, without US support, the natural release of drugs from the hydrogels occurred following diffusion only. The viscoelasticity of the hydrogel matrix indicated that the matrix became somewhat softened after US exposure at 2.5 and 3% CS, but at 1.5 and 2%, the hydrogel matrix became more softened because US forces acted on the deformation of hydrogel and softening occurred.

In actual clinical practice, the effects of US on cells are an important factor. Therefore, to consider the effects of US on fibroblasts in particular, we examined the survival of fibroblasts in response to US exposure in vitro. Fibroblast proliferation was followed in our previous paper.[52] The cells were prepared at a density of 8×10^3 cells cm^{-2} and the cell solution was irradiated with 43 kHz US with different times at different powers, and then their proliferation was examined 12 h later. The results showed that under the irradiation conditions of 10 W US for 10, 30, 60, and 120 min, respectively, the percentage of cell viability after 12 h was 87, 74, 55, and 30%, indicating that prolonged exposure time could cause minor, but not fatal, cell damage. Interestingly, after 2 h of exposure, cell morphology was largely unaffected. Continued investigation is now in progress and in the near future it will be to optimize the US drug release of the hydrogel medicine under conditions that minimize the effects of US on the cells.

AUTHOR INFORMATION

Corresponding Author

Takaomi Kobayashi − *Department of Energy and Environmental Science, Nagaoka University of Technology, Nagaoka, Niigata 940-2188, Japan; Department of Science of Technology Innovation, Nagaoka University of Technology, Nagaoka, Niigata 940-2188, Japan;* orcid.org/0000-0001-7649-4607; Phone: +81-258-47-9326; Email: takaomi@vos.nagaokaut.ac.jp

Authors

Tu Minh Tran Vo − *Department of Energy and Environmental Science, Nagaoka University of Technology, Nagaoka, Niigata 940-2188, Japan; Department of Materials Science, Chulalongkorn University, Faculty of Science, Bangkok 10330, Thailand*

Pranut Potiyaraj − *Department of Materials Science, Chulalongkorn University, Faculty of Science, Bangkok 10330, Thailand;* orcid.org/0000-0002-9114-9155

Patricia del Val − *Department of Mechanics, Design and Industrial Management, University of Deusto, Bilbo, Bizkaia 48007, Spain*

Complete contact information is available at: https://pubs.acs.org/10.1021/acsomega.3c06213

Author Contributions

T.K.: conceptualization, writing—review and editing, supervision; T.M.T.V.: methodology, characterization, writing—original draft; P.P.: supervision. P.d.V.: hydrogel synthesis method.

Notes

The authors declare no competing financial interest.

ACKNOWLEDGMENTS

This work was supported by GAICCE received from the ASEAN University Network/Southeast Asia Engineering Education Development Network (AUN/SEED-Net) for the double-degree programs of Nagaoka University of Technology, Japan and Chulalongkorn University, Thailand, and Overseas Research Experience Scholarship for Graduate Students.

REFERENCES

(1) Qiu, Y.; Park, K. Environment-Sensitive Hydrogels for Drug Delivery. *Adv. Drug Delivery Rev.* **2012**, *64*, 49−60.

(2) Hossen, S.; Hossain, M. K.; Basher, M. K.; Mia, M. N. H.; Rahman, M. T.; Uddin, M. J. Smart Nanocarrier-Based Drug Delivery Systems for Cancer Therapy and Toxicity Studies: A Review. *J. Adv. Res.* **2019**, *15*, 1−18.

(3) Buwalda, S. J.; Vermonden, T.; Hennink, W. E. Hydrogels for Therapeutic Delivery: Current Developments and Future Directions. *Biomacromolecules* **2017**, *18* (2), 316−330.

(4) Van Vlierberghe, S.; Dubruel, P.; Schacht, E. Biopolymer-Based Hydrogels As Scaffolds for Tissue Engineering Applications: A Review. *Biomacromolecules* **2011**, *12* (5), 1387−1408.

(5) Jafarimanesh, M. A.; Ai, J.; Shojaei, S.; Khonakdar, H. A.; Darbemamieh, G.; Shirian, S. Sustained Release of Valproic Acid Loaded on Chitosan Nanoparticles within Hybrid of Alginate/Chitosan Hydrogel with/without Stem Cells in Regeneration of Spinal Cord Injury. *Prog. Biomater.* **2023**, *12*, 75−86.

(6) Hadinugroho, W.; Martodihardjo, S.; Fudholi, A.; Riyanto, S.; Prasetyo, J. Hydroxypropyl Methylcellulose as Hydrogel Matrix and Citric Acid-Locust Bean Gum as Negative Matrix for Controlled Release Tablet. *ACS Omega* **2023**, *8* (8), 7767−7778.

(7) Chaudhary, S.; Chakraborty, E. Hydrogel Based Tissue Engineering and Its Future Applications in Personalized Disease Modeling and Regenerative Therapy. *Beni-Suef Univ. J. Basic Appl. Sci.* **2022**, *11* (1), No. 3.

(8) Casadidio, C.; Peregrina, D. V.; Gigliobianco, M. R.; Deng, S.; Censi, R.; Di Martino, P. Chitin and Chitosans: Characteristics, Eco-

Friendly Processes, and Applications in Cosmetic Science. *Mar. Drugs* **2019**, *17* (6), No. 369.
(9) Putri, T. S.; Rianti, D.; Rachmadi, P.; Yuliati, A. Effect of Glutaraldehyde on the Characteristics of Chitosan−Gelatin−β-Tricalcium Phosphate Composite Scaffolds. *Mater. Lett.* **2021**, *304*, No. 130672.
(10) Sun, J.; Chen, J.; Bi, Y.; Xiao, Y.; Ding, L.; Bai, W. Fabrication and Characterization of β-Cyclodextrin-Epichlorohydrin Grafted Carboxymethyl Chitosan for Improving the Stability of Cyanidin-3-Glucoside. *Food Chem.* **2022**, *370*, No. 130933.
(11) Abdulhameed, A. S.; Jawad, A. H.; Mohammad, A. K. T. Synthesis of Chitosan-Ethylene Glycol Diglycidyl Ether/TiO2 Nanoparticles for Adsorption of Reactive Orange 16 Dye Using a Response Surface Methodology Approach. *Bioresour. Technol.* **2019**, *293*, No. 122071.
(12) Jawad, A. H.; Mamat, N. F. H.; Hameed, B. H.; Ismail, K. Biofilm of Cross-Linked Chitosan-Ethylene Glycol Diglycidyl Ether for Removal of Reactive Red 120 and Methyl Orange: Adsorption and Mechanism Studies. *J. Environ. Chem. Eng.* **2019**, *7* (2), No. 102965.
(13) Shamay, Y.; Adar, L.; Ashkenasy, G.; David, A. Light Induced Drug Delivery into Cancer Cells. *Biomaterials* **2011**, *32* (5), 1377−1386.
(14) Bardajee, G. R.; Hosseini, S. S.; Ghavami, S. Embedded of Nanogel into Multi-Responsive Hydrogel Nanocomposite for Anticancer Drug Delivery. *J. Inorg. Organomet. Polym. Mater.* **2018**, *28* (6), 2196−2205.
(15) Don, T.-M.; Huang, M.-L.; Chiu, A.-C.; Kuo, K.-H.; Chiu, W.-Y.; Chiu, L.-H. Preparation of Thermo-Responsive Acrylic Hydrogels Useful for the Application in Transdermal Drug Delivery Systems. *Mater. Chem. Phys.* **2008**, *107* (2), 266−273.
(16) Hrubý, M.; Koňák, Č.; Ulbrich, K. Polymeric Micellar PH-Sensitive Drug Delivery System for Doxorubicin. *J. Controlled Release* **2005**, *103* (1), 137−148.
(17) Li, Y.; Xiao, W.; Xiao, K.; Berti, L.; Luo, J.; Tseng, H. P.; Fung, G.; Lam, K. S. Well-Defined, Reversible Boronate Crosslinked Nanocarriers for Targeted Drug Delivery in Response to Acidic PH Values and Cis -Diols. *Angew. Chem.* **2012**, *124* (12), 2918−2923.
(18) Wei, P.; Jan, E.; Jianzhong, C. Ultrasound - Responsive Polymer - Based Drug Delivery Systems. *Drug Delivery Transl. Res.* **2021**, *11*, 1323−1339.
(19) Ninomiya, K.; Kawabata, S.; Tashita, H.; Shimizu, N. Ultrasound-Mediated Drug Delivery Using Liposomes Modified with a Thermosensitive Polymer. *Ultrason. Sonochem.* **2014**, *21* (1), 310−316.
(20) Holowka, E. P.; Bhatia, S. K. Smart Drug Delivery Systems. In *Drug Delivery*; Springer: New York, NY, 2014; pp 265−316.
(21) Chen, D.; Wu, J. An in Vitro Feasibility Study of Controlled Drug Release from Encapsulated Nanometer Liposomes Using High Intensity Focused Ultrasound. *Ultrasonics* **2010**, *50* (8), 744−749.
(22) Pitt, W. G.; Husseini, G. A.; Staples, B. J. Ultrasonic Drug Delivery − a General Review. *Expert Opin. Drug Delivery* **2004**, *1* (1), 37−56.
(23) Klibanov, A. L.; Hossack, J. A. Ultrasound in Radiology: From Anatomic, Functional, Molecular Imaging to Drug Delivery and Image-Guided Therapy. *Invest. Radiol.* **2015**, *50* (9), 657−670.
(24) Kobayashi, T. Cellulosic Medicine Hydrogels with Cyto- and Biocompatible Properties for Ultrasound Stimuli-Drug Release Materials. In *Materials for Biomedical Engineering*; Elsevier Inc., 2019; pp 165−181.
(25) Jiang, H.; Kobayashi, T. Ultrasound Stimulated Release of Gallic Acid from Chitin Hydrogel Matrix. *Mater. Sci. Eng., C* **2017**, *75*, 478−486.
(26) Moyano, D. B.; Paraiso, D. A.; González-Lezcano, R. A. Possible Effects on Health of Ultrasound Exposure, Risk Factors in the Work Environment and Occupational Safety Review. *Healthcare* **2022**, *10*, No. 423.
(27) Polat, B. E.; Hart, D.; Langer, R.; Blankschtein, D. Ultrasound-Mediated Transdermal Drug Delivery: Mechanisms, Scope, and Emerging Trends. *J. Controlled Release* **2011**, *152* (3), 330−348.
(28) Mitragotri, S. Healing Sound: The Use of Ultrasound in Drug Delivery and Other Therapeutic Applications. *Nat. Rev. Drug Discovery* **2005**, *4* (3), 255−260.
(29) Cotero, V.; Graf, J.; Miwa, H.; Hirschstein, Z.; Qanud, K.; Huerta, T. S.; Tai, N.; Ding, Y.; Jimenez-Cowell, K.; Tomaio, J. N.; Song, W.; Devarajan, A.; Tsaava, T.; Madhavan, R.; Wallace, K.; Loghin, E.; Morton, C.; Fan, Y.; Kao, T. J.; Akhtar, K.; Damaraju, M.; Barenboim, L.; Maietta, T.; Ashe, J.; Tracey, K. J.; Coleman, T. R.; Di Carlo, D.; Shin, D.; Zanos, S.; Chavan, S. S.; Herzog, R. I.; Puleo, C. Stimulation of the Hepatoportal Nerve Plexus with Focused Ultrasound Restores Glucose Homoeostasis in Diabetic Mice, Rats and Swine. *Nat. Biomed. Eng.* **2022**, *6* (6), 683−705.
(30) Daffertshofer, M.; Fatar, M. Therapeutic Ultrasound in Ischemic Stroke Treatment: Experimental Evidence. *Eur. J. Ultrasound* **2002**, *16* (1), 121−130.
(31) Diaz-Alejo, J. F.; Gomez, I. G.; Earl, J. Ultrasounds in Cancer Therapy: A Summary of Their Use and Unexplored Potential. *Oncol. Rev.* **2022**, *16* (1), No. 531.
(32) Lattwein, K. R.; Shekhar, H.; Kouijzer, J. J. P.; van Wamel, W. J. B.; Holland, C. K.; Kooiman, K. Sonobactericide: An Emerging Treatment Strategy for Bacterial Infections. *Ultrasound Med. Biol.* **2020**, *46* (2), 193−215.
(33) Kim, Y. J.; Moon, I. J.; Lee, H. W.; Won, C. H.; Chang, S. E.; Lee, M. W.; Choi, J. H.; Lee, W. J. The Efficacy and Safety of Dual-Frequency Ultrasound for Improving Skin Hydration and Erythema in Patients with Rosacea and Acne. *J. Clin. Med.* **2021**, *10*, No. 834.
(34) Warden, S. J.; Fuchs, R. K.; Kessler, C. K.; Avin, K. G.; Cardinal, R. E.; Stewart, R. L. Ultrasound Produced by a Conventional Therapeutic Ultrasound Unit Accelerates Fracture Repair. *Phys. Ther.* **2006**, *86* (8), 1118−1127.
(35) Gunbas, I. D.; Sezer, U. A.; Gülce İz, S.; Gürhan, İ. D.; Hasirci, N. Semi-IPN Chitosan/PEG Microspheres and Films for Biomedical Applications: Characterization and Sustained Release Optimization. *Ind. Eng. Chem. Res.* **2012**, *51* (37), 11946−11954.
(36) Baghbani, F.; Chegeni, M.; Moztarzadeh, F.; Hadian-Ghazvini, S.; Raz, M. Novel Ultrasound-Responsive Chitosan/Perfluorohexane Nanodroplets for Image-Guided Smart Delivery of an Anticancer Agent: Curcumin. *Mater. Sci. Eng., C* **2017**, *74*, 186−193.
(37) Cheung, H. K.; Han, T. T. Y.; Marecak, D. M.; Watkins, J. F.; Amsden, B. G.; Flynn, L. E. Composite Hydrogel Scaffolds Incorporating Decellularized Adipose Tissue for Soft Tissue Engineering with Adipose-Derived Stem Cells. *Biomaterials* **2014**, *35* (6), 1914−1923.
(38) Ji, X.; Shao, H.; Li, X.; Ullah, M. W.; Luo, G.; Xu, Z.; Ma, L.; He, X.; Lei, Z.; Li, Q.; Jiang, X.; Yang, G.; Zhang, Y. Injectable Immunomodulation-Based Porous Chitosan Microspheres/HPCH Hydrogel Composites as a Controlled Drug Delivery System for Osteochondral Regeneration. *Biomaterials* **2022**, *285*, No. 121530.
(39) Xu, J.; Strandman, S.; Zhu, J. X. X.; Barralet, J.; Cerruti, M. Genipin-Crosslinked Catechol-Chitosan Mucoadhesive Hydrogels for Buccal Drug Delivery. *Biomaterials* **2015**, *37*, 395−404.
(40) Zhou, Y.; Ma, G.; Shi, S.; Yang, D.; Nie, J. Photopolymerized Water-Soluble Chitosan-Based Hydrogel as Potential Use in Tissue Engineering. *Int. J. Biol. Macromol.* **2011**, *48* (3), 408−413.
(41) Sirsi, S. R.; Borden, M. A. State-of-the-Art Materials for Ultrasound-Triggered Drug Delivery. *Adv. Drug Delivery Rev.* **2014**, *72*, 3−14.
(42) Zhang, Y.; Tachibana, R.; Okamoto, A.; Azuma, T.; Sasaki, A.; Yoshinaka, K.; Tei, Y.; Takagi, S.; Matsumoto, Y. Ultrasound-Mediated Gene Transfection in Vitro: Effect of Ultrasonic Parameters on Efficiency and Cell Viability. *Int. J. Hyperthermia* **2012**, *28* (4), 290−299.
(43) Tallarida, R. J. Amoxicillin. In *TOP 200*; Springer New York: New York, NY, 1982; pp 18−19.
(44) Iresha, H.; Kobayashi, T. Ultrasound-Triggered Nicotine Release from Nicotine-Loaded Cellulose Hydrogel. *Ultrason. Sonochem.* **2021**, *78*, No. 105710.
(45) Yang, H. M.; Won, Y. H.; Yoon, H. Y.; Kim, C. H.; Goo, Y. T.; Chang, I. H.; Choi, Y. W. Screening of Polymer Additives in

https://doi.org/10.1021/acsomega.3c06213
ACS Omega 2024, 9, 585−597

Poloxamer 407 Hydrogel Formulations for Intravesical Instillation: Evaluation of Mechanical Properties, Gel-Forming Capacity, and Drug Release. *Polymer* **2020**, *44* (6), 817−826.
(46) Sanchez-Rexach, E.; de Arenaza, I. M.; Sarasua, J. R.; Meaurio, E. Antimicrobial Poly(ε-Caprolactone)/Thymol Blends: Phase Behavior, Interactions and Drug Release Kinetics. *Eur. Polym. J.* **2016**, *83*, 288−299.
(47) Bruschi, M. L.Mathematical Models of Drug Release. In *Strategies to Modify the Drug Release from Pharmaceutical Systems*; Woodhead Publishing, 2015; pp 63−86.
(48) Peppas, N. A.; Narasimhan, B. Mathematical Models in Drug Delivery: How Modeling Has Shaped the Way We Design New Drug Delivery Systems. *J. Controlled Release* **2014**, *190*, 75−81.
(49) Franzén, H. M.; Draget, K. I.; Langebäck, J.; Nilsen-Nygaard, J. Characterization and Properties of Hydrogels Made from Neutral Soluble Chitosans. *Polymers* **2015**, *7* (3), 373−389.
(50) Jiang, H.; Tovar-Carrillo, K.; Kobayashi, T. Ultrasound Stimulated Release of Mimosa Medicine from Cellulose Hydrogel Matrix. *Ultrason. Sonochem.* **2016**, *32*, 398−406.
(51) Noguchi, S.; Takaomi, K. Ultrasound Response of Viscoelastic Changes of Cellulose Hydrogels Triggered with Sono-Deviced Rheometer. *Ultrason. Sonochem.* **2020**, *67*, No. 105143.
(52) Tovar-Carrillo, K. L.; Sueyoshi, S. S.; Tagaya, M.; Kobayashi, T. Fibroblast Compatibility on Scaffold Hydrogels Prepared from Agave Tequilana Weber Bagasse for Tissue Regeneration. *Ind. Eng. Chem. Res.* **2013**, *52* (33), 11607−11613.

https://doi.org/10.1021/acsomega.3c06213
ACS Omega 2024, 9, 585−597